

# Exchange in a silicon-based quantum dot quantum computer architecture

S.N. Coppersmith

*Department of Physics, University of Wisconsin, Madison, Wisconsin 53706*

Seungwon Lee and Paul von Allmen

*Jet Propulsion Laboratory, California Institute of Technology, Pasadena, California 91109*

In bulk silicon, intervalley electronic interference has been shown to lead to strong oscillations in the exchange coupling between impurity electronic wavefunctions, posing a serious manufacturability problem for proposed quantum computers. Here we show that this problem does not arise in proposed architectures using Si/SiGe quantum dots because of the large in-plane strain in Si quantum wells together with the strong confinement potential typical of heterostructures.

PACS numbers: 03.67.Lx, 73.21.Fg, 73.21.La

**Introduction.** The proposal to build a quantum computer with qubits that are single electrons confined in gated silicon quantum dots in silicon/silicon-germanium heterostructures [1, 2] is attractive because of the self-aligning properties of quantum dots as well as the long coherence times of electron spins in silicon [4, 5]. However, one complication of silicon compared to a direct band gap material such as gallium arsenide is the valley degeneracy in the band structure. As Refs. [6, 7, 8, 9] point out, interference between valleys causes charge oscillations that can cause the coupling between qubits to vary rapidly in space. Since the fundamental two-qubit gate is achieved by varying the overlap of electron wavefunctions centered at different locations, obtaining reliable gates would appear to require controlling the individual wavefunctions on the scale of the oscillations and not the much longer length scale describing the variation of the envelope of the wavefunctions. This sensitivity has severe implications for the feasibility of constructing a reliable quantum computer using silicon.

Here we present theoretical arguments and atomistic simulations that show that the large in-plane strain present in a silicon quantum well, together with the strong potential confining electrons in the quantum well, combine to eliminate the problem of the fast oscillations in the overlap of wavefunctions of electrons centered at different locations in a Si quantum well in a Si/SiGe heterostructure. The result depends on the strong heterostructure confinement present in the gated quantum dot architecture, and does not apply to other Si-based quantum computing schemes [10, 11, 12].

**Effect of Strain on Electron Wavefunctions in Si Quantum Wells.** Unlike gallium arsenide, unstrained silicon has six-fold degenerate conduction band minima located along the [100], [010], and [001] directions, about 85% of the way to the boundary of the Brillouin zone. Interference between these valleys causes fast oscillations in

the electron density, on the scale of the interatomic spacing. In bulk silicon the oscillations occur along the  $x$ ,  $y$ , and  $z$  directions. These fast oscillations make controlling the exchange coupling accurately, which is necessary to make a two-qubit gate [13], much more difficult [6, 7, 8].

In Si/SiGe heterostructures the large in-plane strain present in the quantum well reduces the six-fold valley degeneracy to a four-fold and a two-fold one. For a typical quantum well in the  $x$ - $y$  plane, perpendicular to the [001] crystal axes, the two lowest energy valleys are at  $k_x = 0$ ,  $k_y = 0$ , and  $\pm k_z$ , with  $k_z \neq 0$ . For typical heterostructures, the minima with nonzero  $k_x$  or  $k_y$  have energies more than 0.1 eV higher than the minima with nonzero  $k_z$ , so that at the low temperatures at which a quantum computer would operate, only the valleys with  $k_x = k_y = 0$  are relevant. [7, 8, 14] Therefore, in the plane of the quantum well the charge density does not oscillate. However, the two degenerate valleys along  $\pm k_z$  do lead to oscillations along the  $z$  direction. Therefore, strain alone does not completely remove the extreme sensitivity of the exchange coupling to small changes in position, especially for impurity based qubits [7, 8].

Below we show that in a Si/SiGe quantum dot quantum computer wavefunction oscillations along  $z$  do not lead to problems with controllability of the exchange interaction because the oscillations of the wavefunctions of different qubits are aligned by the strong confinement potential of the quantum well. The argument is quite general, and the result is robust even in the presence of gate potential fluctuations and imperfections such as quantum well width variations.

**Role of Confinement Potential.** The exchange interaction does not exhibit fast oscillations in quantum wells because the oscillations along  $z$  are aligned by the strong quantum well potential. The physical reason for the alignment of the charge density oscillations perpendicular to the quantum well plane is that the quan-

tum well confinement potential varies on a much shorter length scale than any in-plane potential variations. (Recall that typical quantum wells have 10 nm widths and potential steps occurring on the single unit cell scale and heights  $\gtrsim 0.1$  eV [15], while the potentials defining the quantum dot vary on length scales of many tens of nanometers.) Because of this separation of length scales, it is appropriate to use the Born-Oppenheimer (B-O) approximation [16, 17]. We wish to find the lowest energy eigenstate  $\psi_E$  of the time-independent Schrödinger equation of an electron in a single quantum well,

$$\left[ -\frac{\hbar^2}{2m} \left( \frac{\partial^2}{\partial x^2} + \frac{\partial^2}{\partial y^2} + \frac{\partial^2}{\partial z^2} \right) + V(x, y, z) \right] \psi_E(x, y, z) = E\psi_E(x, y, z). \quad (1)$$

We write the potential  $V(x, y, z)$  as the sum of three contributions, the atomic potential  $V_a(x, y, z)$ , the confinement potential  $V_c(x, y, z)$ , and the residual potential  $V_r(x, y, z)$ , which accounts for potentials from external gates and possible weak impurity potentials (e.g., from dopant inhomogeneities in the modulation doping layer). For simplicity, initially we will ignore the atomic potential  $V_a(x, y, z)$  and consider a system with confinement and residual potentials whose sum varies much quickly along the  $z$  direction than in the  $x - y$  plane. We follow the usual B-O argument [16, 18] and write  $\psi(x, y, z) = \Phi_0(z; x, y)\chi(x, y)$ , where  $\Phi_0(z; x, y)$  describes the ground state wavefunction as a function of  $z$  at given  $x$  and  $y$ , and  $\chi(x, y)$  describes the in-plane variations. The B-O prescription is to first find  $\Phi_0$  by solving

$$\left[ -\frac{\hbar^2}{2m} \frac{d^2}{dz^2} + V(x, y, z) \right] \Phi_0(z; x, y) = V_{eff}(x, y)\Phi_0(z; x, y), \quad (2)$$

and then determine  $\chi(x, y)$  from

$$\left[ -\frac{\hbar^2}{2m} \left( \frac{\partial^2}{\partial x^2} + \frac{\partial^2}{\partial y^2} \right) + V_{eff}(x, y) \right] \chi(x, y) = E\chi(x, y). \quad (3)$$

Eq. (2) for the  $z$ -dependence of the wavefunction depends only on the local value of  $x$  and  $y$ . The wavefunctions obtained for two different residual potentials in the  $x - y$  plane,  $V_{r1}(\vec{r})$  and  $V_{r2}(\vec{r})$  (corresponding to electrons centered on two different quantum dots), are  $\Phi_0(z; x, y)\chi_1(x, y)$  and  $\Phi_0(z; x, y)\chi_2(x, y)$ . Here,  $\chi_1$  and  $\chi_2$  are distinct, but  $\Phi_0$  is the same for the two wavefunctions. Therefore, while the wavefunction can vary quickly as a function of  $z$ , this  $z$ -dependence is identical for wavefunctions centered at different locations in the  $x - y$  plane. The overlap matrix element between electrons centered at  $\vec{r}_1$  and  $\vec{r}_2$ ,  $\langle \vec{r}_1 | \vec{r}_2 \rangle$  is

$$\langle \vec{r}_1 | \vec{r}_2 \rangle = \int dx dy \chi_1^*(x, y)\chi_2(x, y) \left[ \int dz |\Phi_0(z; x, y)|^2 \right]. \quad (4)$$

The term in brackets does not depend on the residual potential  $V_r(x, y)$ , so it does not change when the gate potentials are varied. In other words, the strong quantum well confinement “locks” the variations perpendicular to the quantum well plane. Since, as discussed above, the wavefunctions in these strained quantum wells have no oscillations in the  $x - y$  plane, the scale of all variations in the exchange coupling is the quantum dot size, typically of order at least 100 nm. Therefore, the valley degeneracy does not lead to additional problems in controlling the exchange interaction in a Si/SiGe quantum dot computer.

To include the atomic potential  $V_a(x, y, z)$ , we use the envelope approximation [19] and write the wavefunction

$$\psi(\vec{r}) = \sum_{j=1}^2 \alpha_j F_j(\vec{r}) u_j(\vec{r}) e^{i\vec{k}_j \cdot \vec{r}_j}, \quad (5)$$

where  $u_j(\vec{r}) e^{i\vec{k}_j \cdot \vec{r}_j}$  is the Bloch wave at the minimum of the  $j^{\text{th}}$  valley, the  $\alpha_j$  describe the amplitude of the contribution from each valley, and the  $F_j(\vec{r})$  are “envelope” functions. Because band offsets in typical heterostructures are  $\lesssim 0.2$  eV, while atomic potentials are several eV, the variations induced by the confinement potential are much slower than those induced by the atomic potential, and therefore the envelope function itself satisfies the Schrödinger equation, Eq. (1) [19]. Thus, within the envelope approximation, the argument given above with no atomic potential applies with no modifications.

In conclusion, we have shown that the strong confinement potential in Si/SiGe quantum wells causes the exchange coupling to depend smoothly on quantum dot separation.

**Tight-Binding Model Calculation.** In explicit support of the aforementioned conclusions we have numerically computed the behavior of the exchange coupling as a function of the separation between quantum dots in Si/SiGe heterostructures by using the quantitative nano-electronic modeling tool NEMO-3D [20]. NEMO-3D describes the electron Hamiltonian in the framework of an  $sp^3d^5s^*$  nearest-neighbor empirical tight-binding model, which allows us to incorporate explicitly the effect of well-width variation, interface roughness, and strain at the atomic level. The atomistic description is essential to verify the aforementioned argument that the electron wave function varies smoothly in the  $x - y$  plane without fast oscillations at the atomic scale. We use the empirical tight-binding parameters of Ref. [21], which reproduce both the band edges and effective masses of the lowest conduction band and the highest valence band to within less than 5%. The effects of strain on the band edges and effective masses are incorporated

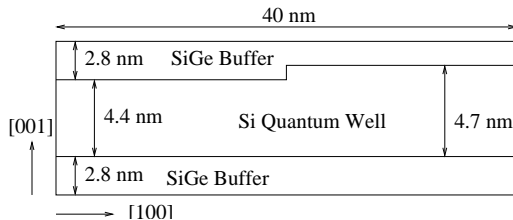


FIG. 1: Schematic cross section of the modeled system which consists of a Si quantum well with a width of 4.4 nm and a  $\text{Si}_{0.7}\text{Ge}_{0.3}$  barrier material with a width of 2.8 nm below and above the Si well. The width of one half of the Si well is increased by one monolayer to imitate a well-width variation arising from growth inhomogeneity.

into the model by modifying the tight-binding parameters with the Löwdin orthogonalization procedure, the Slater-Koster table, and the generalized version of the Harrison's  $d^{-2}$  scaling law [22].

Figure 1 shows the modeled system, a strained Si quantum well with a width of 4.4 nm and a relaxed  $\text{Si}_{0.7}\text{Ge}_{0.3}$  barrier buffer with a width of 2.8 nm below and above the Si well. The supercell dimension in the  $x$ - $y$  plane is 40 nm. To simulate the effect of the well-width variation due for example to a miscut substrate, the Si well width is increased by one monolayer in half the supercell in the  $x$  direction. The external gate potential  $V_g(x, y, z)$  for the lateral confinement is approximated by a harmonic potential in the  $x - y$  plane and a linear potential along the  $z$  direction:  $V_g(x, y, z) = A(x^2 + y^2) + Bz$ , with  $A$  and  $B$  chosen to be  $0.1 \text{ meV/nm}^2$  and  $20 \text{ meV/nm}$ , respectively, in agreement with electrostatic potential calculations [24]. All other potentials  $V_c(x, y, z)$  and  $V_a(x, y, z)$  are included in the tight-binding Hamiltonian via the couplings between the tight-binding basis orbitals. By diagonalizing the resulting Hamiltonian, the ground state electron wave function  $\psi(\vec{r})$  for a single quantum dot is obtained. The two-electron wave functions in a system of two quantum dots are prepared by superposing the single electron wave functions centered at each of the two quantum dots. Two types of two-electron wave functions can be constructed: symmetric and antisymmetric states.

The exchange coupling  $J$  of the two-electron system or, equivalently, the energy difference between the symmetric and antisymmetric states is given approximately by [6]

$$J(\vec{R}) = \int dx_1 dy_1 dz_1 dx_2 dy_2 dz_2 \psi^*(\vec{r}_1) \psi^*(\vec{r}_2 - \vec{R}) \frac{e^2}{\epsilon |\vec{r}_1 - \vec{r}_2|} \psi(\vec{r}_1 - \vec{R}) \psi(\vec{r}_2), \quad (6)$$

where  $\vec{R}$  is the relative distance vector between the cen-

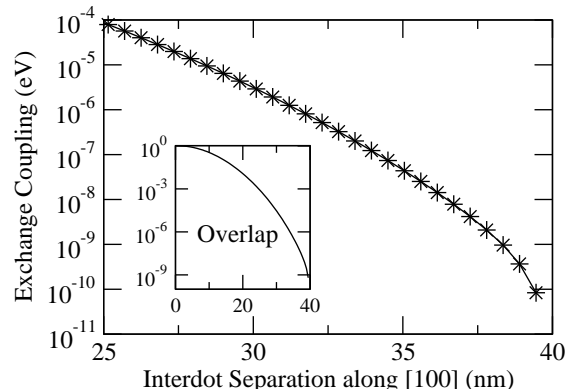


FIG. 2: Exchange coupling as a function of the interdot separation along the  $[100]$  direction for two quantum dots that are electrostatically defined in a Si quantum well surrounded by a  $\text{Si}_{0.7}\text{Ge}_{0.3}$  buffer. The inset shows the overlap between single-electron wave functions  $\psi(\mathbf{r})$  centered at each of the two quantum dots, i.e.  $|\int dx dy dz \psi^*(\vec{r}-X)\psi(\vec{r})|^2$ , as a function of the interdot separation  $X$  along the  $[100]$  direction. Both the exchange coupling and the overlap (inset) smoothly increase as the interdot separation decreases. This result clearly demonstrates the absence of atomic-level oscillations.

ters of the two quantum dots and  $\epsilon$  is the dielectric constant. [3] This exchange integral is further expanded into integrals involving tight-binding basis orbitals. The details of the expansion and the calculation of the integrals can be found elsewhere [23].

Figure 2 shows the exchange coupling as a function of the interdot separation along the  $[100]$  direction. As the interdot separation decreases, the exchange coupling smoothly increases without atomic-level oscillations. To show the origin of this behavior, we also plot the overlap between single-electron wave functions centered at each of the two quantum dots in the inset of Fig. 2. As expected, the overlap smoothly increases with the decrease of the interdot separation. These results clearly demonstrate the absence of atomic-level oscillations in the single-electron wave function, and consequently the absence of fast oscillations in the exchange coupling in the two-electron wave function.

**Summary.** We have shown that the exchange interaction between two qubits composed of quantum dots in a Si/SiGe heterostructure exhibits a smooth dependence on qubit separation. The origin of the difference between the behavior in quantum dots and in bulk silicon impurities is the strain and the strong confining potential in the heterostructure.

**Acknowledgements.** We thank the entire UW Solid State Quantum Computing group, and particularly Mark Eriksson, Mark Friesen, Bob Joynt, and Don Savage,

for extremely useful conversations. We also thank all the developers of NEMO-3D for their contributions to this quantum modeling tool. We gratefully acknowledge support from the NSF under Grants DMR-0209630 and DMR-0325634, and by ARDA, ARO, and NSA.

- 
- [1] R. Vrijen, E. Yablonovitch, K. Wang, H. Jiang, A. Balandin, V. Roychowdhury, T. Mor, and D. DiVincenzo, Phys. Rev. A **62**, 012306 (2000).
- [2] M. Friesen, P. Rugheimer, D.E. Savage, M.G. Lagally, D.W. van der Weide, R. Joynt, and M.A. Eriksson, Phys. Rev. B **67**, 121301 (2003).
- [3] The validity of this approximation has been verified in detail via ab initio simulations in Ref. [8].
- [4] G. Feher and E.A. Gere, Phys. Rev. **114**, 1245-1256 (1959).
- [5] A.M. Tyryshkin, S.A. Lyon, A.V. Astashkin, A.M. Rait-simring, Physical Review B **68**, 193207 (2003).
- [6] Belita Koiller, Xuedong Hu, S. Das Sarma, Phys. Rev. Lett. **88**, 027903 (2002).
- [7] Belita Koiller, Xuedong Hu, S. Das Sarma, Phys. Rev. B **66**, 115201 (2002).
- [8] Belita Koiller, R.B. Capaz, Xuedong Hu, S. Das Sarma, to be published in Physical Review B, preprint cond-mat/0402266.
- [9] C.J. Wellard, L.C.L. Hollenberg, F. Parisoli, L.M. Kettle, H.-S. Goan, J.A.L. McIntosh, and D.N. Jamieson, Phys. Rev. B **68**, 195209 (2003).
- [10] B. Kane, Nature (London) **393**, 133 (1998).
- [11] J.L. O'Brien, S.R. Schofield, M.Y. Simmons, R.G. Clark, A.S. Dzurak, N.J. Curson, B.E. Kane, N.S. McAlpine, M.E. Hawley, and G.W. Brown, Phys. Rev. B **64**, 161401(R) (2001).
- [12] T.D. Ladd, J.R. Goldman, F. Yamaguchi, Y. Yamamoto, E. Abe, and K.M. Itoh, Phys. Rev. Lett. **89**, 017901 (2002).
- [13] D. Loss and D.P. DiVincenzo, Phys. Rev. A **57**, 120 (1998).
- [14] C. Tahan, M. Friesen, and R. Joynt, Phys. Rev. B **66**, 035314 (2002).
- [15] F. Schaffler, Semicond. Sci. Technol. **12**, 1515 (1997).
- [16] M. Born and R. Oppenheimer, Ann. Phys. (Leipzig) **84**, 457-484 (1927).
- [17] F. Bentosela, P. Exner, and V.A. Zagrebnov, Phys. Rev. B **57**, 1382-1385 (1998).
- [18] D. Chandler, *Introduction to Modern Statistical Mechanics*, Oxford University Press, New York (1987), pp. 107-108.
- [19] W. Kohn, in *Solid State Physics*, ed. F. Seitz and D. Turnbull (Academic Press, New York, 1957), Vol. 5, p. 257.
- [20] G. Klimeck, F. Oyafuso, T.B. Boykin, R.C. Bowen, and P. von Allmen, Computer Modeling in Engineering and Science **3**, 601 (2002); NEMO-3D is open software, and is available at [http://www.openchannelfoundation.org/projects/NEMO\\_3D](http://www.openchannelfoundation.org/projects/NEMO_3D).
- [21] T.B. Boykin, G. Klimeck, R.C. Bowen, and F. Oyafuso, Phys. Rev. B **66**, 125207 (2002).
- [22] T.B. Boykin, G. Klimeck, and F. Oyafuso, Phys. Rev. B **69**, 115201 (2004).
- [23] S. Lee, L. Jönsson, J. W. Wilkins, G. Bryant and G. Klimeck, Phys. Rev. B **63**, 195318 (2001).
- [24] M. Friesen, P. Rugheimer, D.E. Savage, M.G. Lagally, D.W. van der Weide, R. Joynt and M. Eriksson, Phys. Rev. B **67**, 121301 (2003).